Scalable and Iterative Image Super-resolution using DCT Interpolation and Sparse Representation

Saulo R. S. Reis[1] and Graça Bressan[2]

[1]*Dept. of Electrical Engineering, Federal University of Mato Grosso, UFMT, Cuiabá – Mato Grosso, Brazil*
[2]*Dept. of Computing and Digital Systems Engineering, Polytechnic School of the University of São Paulo-EPUSP, São Paulo-SP, Brazil*

Keywords: Super-resolution, Sparse Representation, DCT Interpolation, k-SVD, OMP.

Abstract: In a scenario where acquisition systems have limited resources or available images do not have good quality, super-resolution (SR) techniques are an excellent alternative for improving the image quality. The traditional SR methods proposed in the literature are effective in HR image reconstruction to a magnification factor up to 2. In recent years, example-based SR methods have shown excellent results in the HR image reconstruction to magnification factor 3 or more. In this paper, we propose a scalable and iterative algorithm for single-image SR using a two-step strategy with DCT interpolation and the sparse-based learning method. The method proposed implements some improvements in the dictionary training and the reconstruction process. A new dictionary is built by using an unsharp mask technique for feature extraction. The idea is to reduce the learning time by using two different small dictionaries. The results were compared with others interpolation-based and SR methods and demonstrated the effectiveness of the algorithm proposed in terms of PSNR, SSIM and Visual Quality.

1 INTRODUCTION

Single-image super-resolution (SISR) method use signal processing techniques to reconstruct a high-resolution (HR) image from a set of low-resolution (LR) images. When the acquisition systems have limited resources or available images do not have good quality, SR techniques are an excellent alternative for improving the image quality.

Many important areas have benefited from SR methods so far. In medicine, HR images are used to help doctors to perform more accurate image diagnosis. In remote sensing, HR images provide a better interpretation and analysis of the sensed areas, such as environmental, urban, agriculture, etc. In surveillance systems, HR images can help the police to identify suspects of vandalism or crimes. Other areas that can benefit from high-quality content include Digital TV, restoration of old content for museums and libraries, etc.

SR methods adopt an observation model that includes the effects of the acquisition process such as optical distortion, blurring and noise.

This model can be described as:

$$Y_L = SHX_H + \eta \qquad (1)$$

where Y_L of size $N = N_1 \times N_2$ pixels, represents the observed LR image. X_H denotes the HR image of size $M = M_1 \times M_2$ pixels, with $M > N$. Matrix H of size $M \times M$ represents the effects of the imaging system, such as optical distortion and blurring. Matrix S represents the downsampling operator, and η is zero-mean white noise with variance σ_η^2. The fundamental SR problem is the recovery of HR image X_H from the observed LR image Y_L in (1) without amplifying the effects of noise or blurring.

Traditional SR methods proposed in the literature, such as interpolation-based (Zhang and Xiaoling, 2006; Li and Orchard, 2001; Aly and Dubois, 2005) and reconstruction-based (Park et al, 2003; Zibetti et al, 2011; Baker and Kanade, 2002), have shown effective results in the HR image reconstruction for magnification factors up to 2. However, the image quality degrades rapidly for upper magnification factors. One important alternative to solve this problem is the use of learning-based SR methods (Freeman et al., 2002; Elad and Datsenko, 2009; Qiang et al., 2005; Jian et al., 2003; Jiji and chaudhuri, 2006), that produce a HR image by learning the co-occurrence patterns between LR patches and their corresponding HR patches.

In the last years, many works have addressed the learning-based methods based on the sparse representation of signals. In these methods, each LR image patch can be represented using a linear combination of atoms from an overcomplete dictionary. One of the pioneering works in this direction was proposed by (Yang et al., 2010). Their algorithm is divided into two main steps: a first step of the Dictionary learning using LASSO and OMP algorithms, and a second step of HR image reconstruction. (Zeyde et al., 2010) also considered a similar approach, but with some important modifications. Their method adopted the use of the k-SVD algorithm for dictionary learning and used a pseudo-inverse expression for the HR dictionary construction.

Some works have practiced the idea of using the learning dictionary process according to the structural content of LR and HR patches. In (Dong et al, 2011), the Adaptive Sparse Domain Selection – ASDS algorithm is used for selecting the patches. In (Yang et al., 2012), the patches are grouped into three different sets: soft patches, dominant orientation patches and stochastic patches. In (Zhou et al., 2012), the patches are divided using a Weber Local Descriptor – WLD algorithm. The idea of using a strategy of coupled dictionary training, is presented in (Jia et al., 2013). The coupling is carried out by forcing the sparse HR and LR patches coefficients to have the same number of elements different from zero.

Another emerging approach that has been drawing research in recent years is image interpolation based on DCT transform. (Wu et al., 2010) proposed an Interpolation method for LR video using a hybrid scheme with DCT transform and Wiener filtering. The low frequency coefficients are obtained by the DCT transform and the high frequency coefficients by Wiener Filtering used in the H.264/AVC standard. In this method, the filter coefficients are calculated according to the images of the training set. The SR method proposed in (Garcia et al., 2012), applies DCT interpolation in mixed-resolution videos based on multiple views of the same scene. In (Hung et al., 2011) is proposed the SR method, which the high-frequency coefficients are retrieved using the adjacent high-resolution frames (*key-frames*).

In this paper, we propose a scalable and iterative single-image SR method. The algorithm is based on a two-step strategy that uses the DCT interpolation and sparse representation of signals.

The aim is to improve the high-resolution reconstruction process, including the following contributions:
• A new feature extraction step using an *Unsharp Mask* in order to construct a new LR dictionary;
• Implementation of a scalable and iterative SR process with the HR image obtained from the first iteration, for a news two-step training and HR reconstruction.

The remainder of this paper is organized as follows. In section 2, sparse representation model and DCT interpolation methods are revised. In section 3, we detail the method proposed, composed of two main steps. Experimental results are presented in section 4 and we conclude this paper in section 5.

2 BACKGROUND

2.1 Sparse Representation of Signals

In the sparse representation model, a natural signal can be described as a sparse combination of atoms with respect to an overcomplete dictionary, (Aharon and Bruckstein, 2006). Given a signal $x \in \mathcal{R}^n$ and a dictionary $D \in \mathcal{R}^{n \times k}$ that contains k prototype signal-atoms in columns, the sparsity-based minimization problem is given by:

$$\min_{D,\alpha} \|X - DA\|_2^2 \quad \text{subject to} \quad \|\alpha_i\|_0 \leq T_0 \qquad (2)$$

where $\|.\|_0$ is the l^0 norm, $\|.\|_2$ is the l^2 norm, X is a set of training signals, α_i is a sparse vector and T_0 is target sparsity. Dictionary D can be constructed using a training process from a set of samples, or by prespecified set of functions such as Fourier, Wavelets and Curvelets (Aharon and Bruckstein, 2006). In the SR context, given a set of LR image patches $P_L = \{p_L\}_{i=1}^k$, it can be represented as a sparse combination with respect to LR dictionary D_L. In this case, the optimization problem is given by:

$$\arg \min \|P_L - D_L A\|_0 \quad \text{subject to} \quad \|\alpha_i\|_2^2 \leq T_0 \quad (3)$$

where (3) is minimized iteratively. First, we fix D_L and aim to find the best coefficients of matrix A according to the number of nonzero entries T_0. The second step, the algorithm to search for a better dictionary, according to updated sparse vectors (Aharon and Bruckstein, 2006). An important feature of the sparse representation model is the possibility of using a reduced set of images compared with traditional methods based on learning examples.

2.2 Image Interpolation in the DCT Domain

Image interpolation using DCT transform upscale the image by adding coefficients of zero amplitude in high frequency components of a block (Wu et al, 2010; Hung et al, 2011; Zhang and Chang, 2011; Sun and Cham, 2007). The interpolation process takes an important advantage of DCT domain, that is, to concentrate the frequency coefficients values in regions near the DC components.

First, a LR input image is divided into non-overlapping blocks b_L of size $n \times n$. Then, for each block b_L, a type II DCT transform is applied resulting in a transformed block $B_{L(DCT)}$ as follows:

$$B_{L(DCT)} = DCT_{II}\{b_L\} \tag{4}$$

Then, $B_{L(DCT)}$ is resized according to upscale factor s, by adding zeroes to high frequency components, resulting in a $\hat{B}_{L(DCT)}$ block as follows:

$$\hat{B}_{L(DCT)} = \begin{bmatrix} \{B_{L(DCT)}\}_{n \times n} & \cdots & 0 \\ \vdots & \ddots & \vdots \\ 0 & \cdots & 0 \end{bmatrix}_{sn \times sn} \tag{5}$$

Next, the inverse type III DCT transform is applied to the resized block:

$$\hat{b}_L = IDCT_{III}\{\hat{B}_{L(DCT)}\} \tag{6}$$

where $\hat{b}_L$ is the resulting interpolated block of size $sn \times sn$.

3 PROPOSED SR METHOD

The proposed SR method is divided into two main steps: a first step for training and construction of two LR and HR dictionaries and a second step for reconstructing the HR image, which will be detailed in the sections 3.1 and 3.2.

In addition, we include a new section 3.3, which addresses the iterative and scalable implementation of the proposed method.

3.1 Step 1: Training and Dictionary Construction

First, let a set of HR images of different features in a set be blurred and downsampled, according to equation (1), resulting in an equivalent set of LR images.

For the construction of the LR dictionary D_{L1}, we used a set of four *Laplacian* and G*radient* filters,

with the coefficients given by: $F_1 = [-1,0,1]$, $F_2 = F_1^T$, $F_3 = [1,0,-2,0,1]$ and $F_4 = F_3^T$. These filters are the same used in (Yang et al., 2010; Zeyde et al., 2010). The feature extraction is performed according to the following equation:

$$\tilde{p}_{L1}^i = F_r^i * I_L \tag{7}$$

where " $*$ " denotes convolution operator, $\tilde{p}_{L1}^i$ is the LR patch after the feature extraction process, I_L denotes the LR image of the training set and F_r ($r = 1,2,3,4$) represents the four Laplacian and Gradient filters.

For dictionary D_{L2}, we used an *Unsharp Mask* (Gonzalez and Woods, 2010), as follows:

$$I_{mask} = I_L - I_{L(LP)} \tag{8}$$

with,

$$I_{L(LP)} = H_{LP} * I_L \tag{9}$$

where H_{LP} is low-pass filter and $I_{L(LP)}$ is the smoothed LR image. The idea of using the *Unsharp Mask* is to extract features not present in dictionary D_{L1}. The feature extraction with the unsharp mask produces a new LR patch, given by:

$$\tilde{p}_{L2}^i = F_r^i * [I_L + k.I_{mask}] \tag{10}$$

where I_{mask} represents an unsharp mask image and k is a weight to emphasize the contribution of the unsharp mask. We adopt $k = 1$.

The use of the Laplacian and Gradient filters produce LR patches $\tilde{p}_{L1}^i$ and $\tilde{p}_{L2}^i$ with high dimensionality. In order to reduce the dimensionality, the Principal Analysis Components (PCA) algorithm is applied, using a projection operator denoted by B. The resulting patches are given by:

$$p_{L1}^i = B\tilde{p}_{L1}^i \tag{11}$$

$$p_{L2}^i = B\tilde{p}_{L2}^i \tag{12}$$

Considering LR patches p_{L1}^i and p_{L2}^i, the dictionaries D_{L1} and D_{L2} are constructed using the learning k-SVD and OMP algorithms (Aharon et al., 2006), according to the following equations:

$$\arg min \|p_{L1}^i - D_{L1}\alpha_{1i}\|_2^2 \text{ subject to } \|\alpha_{1i}\| \le T_0 \tag{13}$$

$$\arg min \|p_{L2}^i - D_{L2}\alpha_{2i}\|_2^2 \text{ subject to } \|\alpha_{2i}\| \le T_0 \tag{14}$$

where α_{1i} and α_{2i} represent the sparse vectors with respect to D_{L1} and D_{L2} and T_0 is the target sparsity. In order to reduce the learning time, dictionaries D_{H1} and D_{H2} are obtained by pseudo-inverse expression:

$$D_{H1} = P_{H1}Q_1^T(Q_1Q_1^T)^{-1} \tag{15}$$

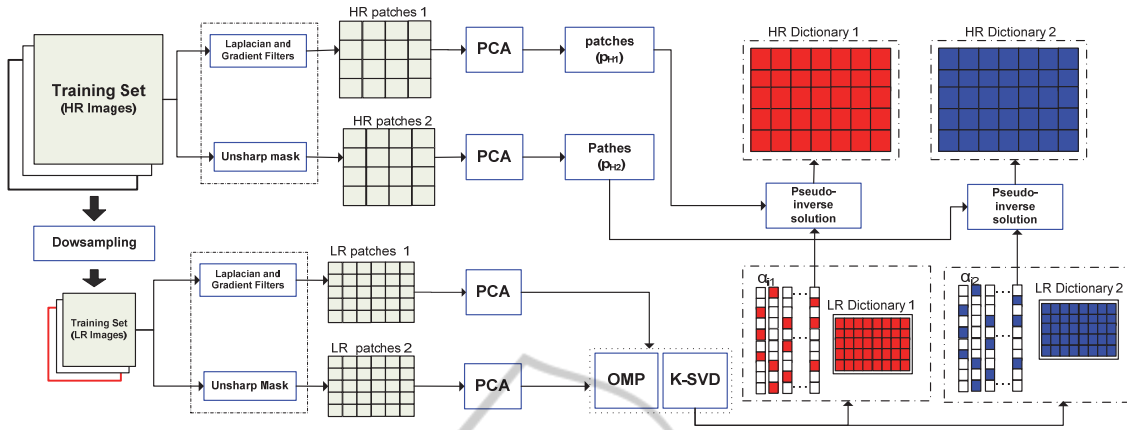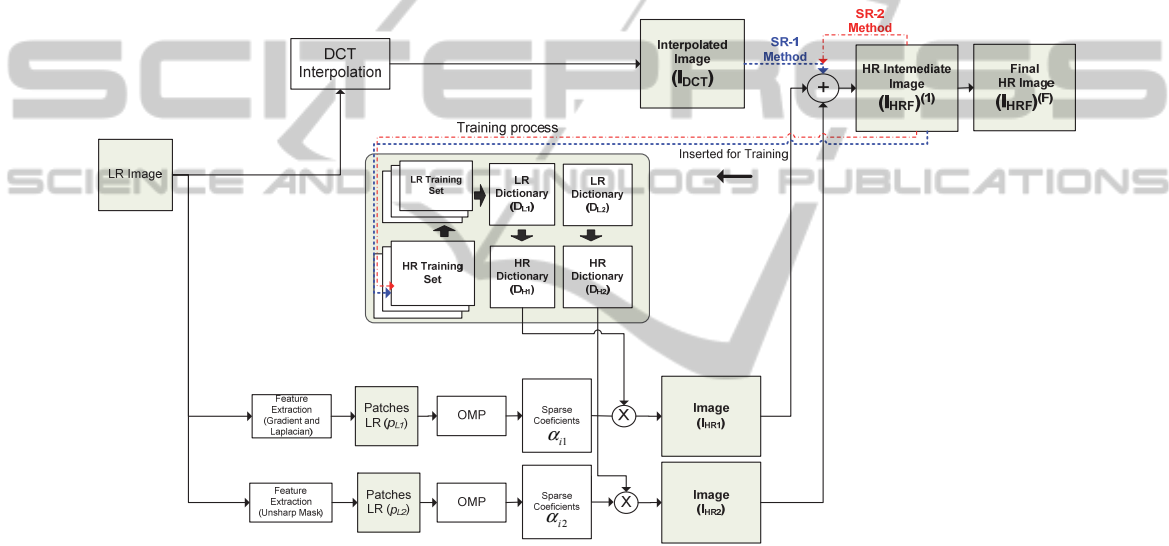$$D_{H2} = P_{H2}Q_2^T(Q_2Q_2^T)^{-1} \tag{16}$$

Figure 1**:** Overview of the Training and dictionary construction step described in section 3.1.

Figure 2**:** Framework of Iterative and scalable single-image SR method. In Both SR-1 and SR-2 implementation, The $(I_{HRF})^1$ image is inserted in the training set for a new scalable and iterative process.

where P_{Hi} $i = 1,2$, represents the matrices built with the HR patches extracted from the training set by using (7) and (10). Q_1 and Q_2 are the matrices that include all the vectors obtained in the sparse coding process. Figure 1 shows an overall framework of the proposed training and dictionary construction step.

3.2 Step 2: HR Image Reconstruction

The HR image is reconstructed with the DCT-based interpolated LR image and the other two images obtained by sparse representation.

First, the input LR image Y_L of size $N_1 \times N_2$ pixels is interpolated with upscale factor s using DCT transform:

$$Y_{DCT}^{LR} = Q_{DCT} Y_L \qquad (17)$$

where Q_{DCT} represents the interpolation operator in the DCT domain described in section 2.2. Also, the LR image Y_L undergoes a feature extraction process by high-pass filtering, using the same process described in section 3.1. By applying this feature extraction process, we get two different types of LR patches, representing different features of the LR image:

$$\tilde{p}_{Y_L1}^i = F_r * Y_L \qquad (18)$$

$$\tilde{p}_{Y_L2}^i = F_r * [Y_L + k.Y_{Lmask}] \qquad (19)$$

Whereas $\tilde{p}_{Y_L1}^i$ and $\tilde{p}_{Y_L2}^i$ have high dimensionality, we also used the PCA algorithm to reduce the dimensionality, resulting in $p_{Y_L1}^i$ and $p_{Y_L2}^i$ patches. Given $p_{Y_L1}^i$, $p_{Y_L2}^i$, D_{L1} and D_{L2}, the proposed algorithm uses a sparse coding algorithm

OMP to calculate the sparse coefficients $\alpha_{Y_L1}^i$ and $\alpha_{Y_L2}^i$, according to equations (13) and (14). Considering sparse coefficients $\alpha_{Y_L1}^i$ and $\alpha_{Y_L2}^i$, the HR patches are obtained by:

$$p_{H1}^i = D_{H1}\alpha_{Y_L1}^i \qquad (20)$$

$$p_{H2}^i = D_{H2}\alpha_{Y_L2}^i \qquad (21)$$

Patches p_{H1}^i and p_{H2}^i are combined with a least squares solution to obtain partial images I_{HR1} and I_{HR2}:

$$I_{HR1} = \left[\sum_i F_r^{i^T} F_r^i\right]^{-1} \sum_i F_r^{i^T} p_{H1}^i \qquad (22)$$

$$I_{HR2} = \left[\sum_i F_r^{i^T} F_r^i\right]^{-1} \sum_i F_r^{i^T} p_{H2}^i \qquad (23)$$

The HR final image consists in the interpolated image DCT Y_{DCT}^{LR} and the two images obtained by the learning process I_{HR1} and I_{HR2} :

$$I_{HRF}^{(F)} = Y_{DCT}^{LR} + \gamma(I_{HR1} + I_{HR2}) \qquad (24)$$

where γ is a factor that represents the contribution of learning Images. In this paper, we adopt $\gamma = 1/2$. A framework of the proposed SR method is presented in Figure 2.

3.3 Scalable and Iterative Implementation

An important contribution of the proposed method is to combine step 1 and step 2 in a scalable and iterative way. The partial HR image $I_{HRF}^{(1)}$ obtained in the first iteration is inserted into the training set to run a new training step. In this case, the final HR image is given by:

$$I_{HRF}^{(n)} = I_{HRF}^{(n-1)} + \frac{1}{2}\left(I_{HR1}^{(n)} + I_{HR2}^{(n)}\right), \ n=2,...,N \quad (25)$$

where N is the number of iterations of the algorithm. The HR image of the first iteration can be inserted in the training set of two ways:

- In the first case, the $I_{HRF}^{(1)}$ image is constructed with the same upscale factor of the final HR image. This image is inserted in the training set for a new step of dictionary training. This case was tested for upscale factor up to 2.

- In the second case, the $I_{HRF}^{(1)}$ image is constructed with an upscale factor smaller than final HR image. This image is inserted in the training set for a new of dictionary training. The high frequency coefficients recovered in $I_{HRF}^{(1)}$ image are transformed into low frequency coefficients in the next iteration of algorithm. For the

simulations tests in section 4, we used an upscale factor 3 to final HR image.

4 EXPERIMENTAL RESULTS

4.1 Simulations Settings

To illustrate the performance of the proposed algorithm, computer simulations were performed in MATLAB® using a computer with Intel Dual Core T4300 2.10 GHz, 3 GB RAM. The images used for the tests were *Cameraman, Jetplane, Lake, Lenna and Living Room*. These images were degraded by blurring and subsampling and then upscaled using factors equal to 3. For training and construction of the LR dictionaries, we used 20 iterations of k-SVD and OMP algorithms. The training set used for the training step, was the same used in (Yang et al, 2010; Zeyde et al, 2010), composed by 92 images that include flowers, landscapes, faces, buildings, in order to extract different features such as edges and textures. However, for the proposed SR algorithm was used only 5 images of the training set.

Apart from inclusion of the HR image in the training set as described in section 3.3, in all simulations, we adopted two configurations for the reconstruction step:

a) **SR-1 algorithm**: the intermediate image $I_{HRF}^{(1)}$ was replaced by the interpolated image Y_{DCT}^{LR} to perform one more iteration of algorithm. This configuration is denoted in Table 1 as **SR-1**.

b) **SR-2 algorithm**: the intermediate image $I_{HRF}^{(1)}$ is updated for each iteration of algorithm. This configuration is denoted in Table 1 as **SR-2**.

The proposed algorithms **SR-1** and **SR-2** was compared with interpolation-based methods such as bicubic and DCT interpolation, and SR methods proposed in (Yang et al, 2010) and (Zeyde et al, 2010).

4.2 Results

Table 1 shows the results in terms of PSNR and SSIM of proposed SR-1 and SR-2 algorithms compared with others SR methods. We can observe that the SR-2 algorithm produced superior results than all others methods. The results indicate that the scalable and iterative strategy using few images of the training set was efficient in the process of reconstruction of HR final image

Figures 3 and 4 show the results of the SR-1 and SR-2 algorithms, considering the quality visual

of the HR image obtained by the methods. We can observe in figures 3(g) and 4(g), that the proposed algorithm SR-2 has recovered more details than others methods. In addition, we observe a minimization of the blocking effects caused by DCT interpolation in the proposed method SR-2.

5 CONCLUSIONS

In this paper, we proposed a novel scalable and iterative single-image SR method using DCT interpolation and sparse representation. The proposed method uses a training strategy of two dictionaries with different high-pass filters to feature extraction and a reduced training set.

Computer simulations demonstrated the effectiveness of the proposed method in terms of PSNR, SSIM and visual quality.

REFERENCES

Aharon, M., Elad, M., Bruckstein, A., 2006. K-SVD: An algorithm for designing overcomplete dictionaries for sparse representation. *IEEE Transactions on Signal Processing*, vol. 54, no. 11, pp. 4311-4322.

Aly H. A., Dubois E., 2005. Image Up-Sampling Using Total-Variation Regularization with a New Observation Model. *IEEE Transactions on Image Processing*, vol. 14, no. 10, pp. 1647-1659.

Baker, S., Kanade, T., 2002. Limits on super-resolution and how to break them. *IEEE Transactions on Pattern Analysis and Machine Intelligence*, vol. 24, no. 9, pp. 1167-1183.

Dong, W., Zhang, L., Shi, G., 2011. Image Deblurring and Super-Resolution by Adaptive Sparse Domain Selection and Adaptive Regularization. *IEEE Transactions on Image Processing*, vol. 20, no. 7, pp. 1838-1857, Jul, 2011.

Elad, M., Datsenko, D., 2009. Example-Based Regularization Deployed to Super-Resolution Reconstruction of a Single Image. *Computer Journal*, vol. 52, no. 1, pp. 15-30.

Freeman, W. T., Jones, T. R., Pasztor, E. C., 2002. Example-based super-resolution. *IEEE Computer Graphics and Applications*, vol. 22, no. 2, pp. 56-65, Mar-Apr.

Garcia, D. C., Dorea, C., Queiroz, R. L., 2012. Super Resolution for Multiview Images Using Depth Information. *IEEE Transactions on Circuits and Systems for Video Technology*, vol. 22, no. 9, pp. 1249-1256.

Gonzalez, R. C., Woods, R. E., 2010. *Digital Image Processing*, Pearson, Third Edition.

Hung, E. M., Garcia, D.C., Queiroz, R.L.D., 2011. Transform domain semi-super resolution. *in ICIP'11*, pp. 1193-1196.

Jia, K. , Wang, X. , Tang, X., 2013. Image Transformation Based on Learning Dictionaries across Image Spaces. *IEEE Transactions on Pattern Analysis and Machine Intelligence*, vol. 35, no. 2, pp. 367-380.

Jian, S., Nan-Ning, Z., Hai, T., 2003. Image hallucination with primal sketch priors. *Proceedings. 2003 IEEE Computer Society Conference on Computer Vision and Pattern Recognition.* pp. II-729-36 vol.2.

Jiji, C. V. Chaudhuri S., 2006. Single-frame image super-resolution through contourlet learning. *Eurasip Journal on Applied Signal Processing*, 2006.

Li X., Orchard M., 2001. New Edge-Directed Interpolation. *IEEE Transactions on Image Processing.* vol. 10, no. 10, pp. 1521-1527.

Park, S. C., Park, M. K., Kang, M. G., 2003. Super-resolution image reconstruction: A technical overview. *IEEE Signal Processing Magazine*, vol. 20, no. 3, pp. 21-36.

Qiang, W., Xiaoou, T., Shum, H., 2005. Patch based blind image super resolution. *Tenth IEEE International Conference on Computer Vision, 2005. ICCV 2005*, pp. 709-716 Vol. 1.

Sun, D., Cham, W. K., 2007. Postprocessing of low bit-rate block DCT coded images based on a fields of experts prior. *IEEE Transactions on Image Processing*, vol. 16, no. 11, pp. 2743-2751.

Wu, Z., Yu, H., Chen, C. W., 2010. A New Hybrid DCT-Wiener-Based Interpolation Scheme for Video Intra Frame Up-Sampling. *IEEE Signal Processing Letters*, vol. 17, no. 10.

Yang, J., Wright, J., Huang, T. S., 2010. Image Super-Resolution Via Sparse Representation. *IEEE Transactions on Image Processing*, vol. 19, no. 11.

Yang, S., Wang M., Chen Y., 2012. Single-Image Super-Resolution Reconstruction via Learned Geometric Dictionaries and Clustered Sparse Coding. *IEEE Transactions on Image Processing*, vol. 21, no. 9, pp. 4016-4028.

Zeyde R., Elad, M., Protter, and M. 2010. On single image scale-up using sparse-representations. *Proceedings of the 7th international conference on Curves and Surfaces.* pp 711-730.

Zhang, W., Cham, W. K., 2011. Hallucinating Face in the DCT Domain. *IEEE Transactions on Image Processing*, vol. 20, no. 10, pp 2769-2779.

Zhang L., Xiaoling W., 2006. An Edge-Guided Image Interpolation Algorithm via Directional Filtering and Data Fusion. *IEEE Transactions on Image Processing*, vol. 15, no. 8, pp. 2226-2238.

Zhou F., Yang, W. Liao, Q., 2012. Single Image Super-Resolution Using Incoherent Sub-dictionaries Learning. *IEEE Transactions on Consumer Electronics*, vol. 58, no. 3, pp. 891-897.

Zibetti, M. V. W., Bazan, F. S. V. Mayer, J., 2011, Estimation of the parameters in regularized simultaneous super-resolution. *Pattern Recognition Letters*, vol. 32, no. 1, pp. 69-78.

APPENDIX

Table 1: PSNR and SSIM Results for upscale 3 and 20 iterations of k-SVD and OMP algorithms.

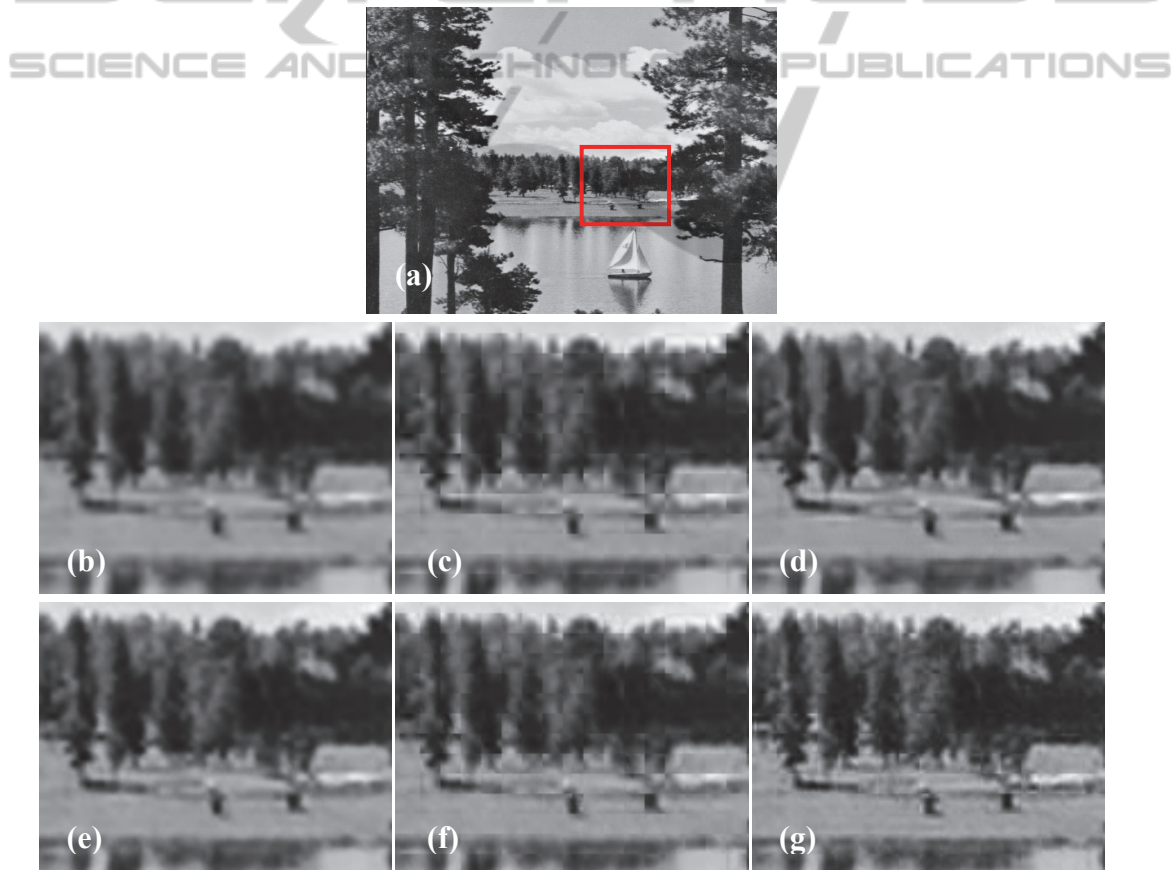| Image	Metric	Bicubic Interpolation	DCT Interpolation	SR Method (YANG et al., 2010)	SR Method (ZEYDE et al., 2010)	Proposed Method SR-1	Proposed Method SR-2
Cameraman	PSNR	30.367	30.299	32.018	32.620	32.0563	**33.987**
	SSIM	0.9587	0.9640	0.959	0.974	0.969	**0.984**
Jetplane	PSNR	29.429	29.313	30.383	30.980	29.976	**31.311**
	SSIM	0.957	0.961	0.956	0.971	0.965	**0.968**
Lake	PSNR	27.419	27.414	28.063	28.556	27.917	**29.599**
	SSIM	0.938	0.937	0.944	0.956	0.949	**0.971**
Lenna	PSNR	31.704	31.622	32.668	33.029	33.436	**33.565**
	SSIM	0.953	0.958	0.956	0.966	0.970	**0.977**
Living Room	PSNR	26.840	26.834	27.441	27.608	27.327	**28.537**
	SSIM	0.893	0.904	0.912	0.920	0.914	**0.956**

Figure 3: Visual quality results for *Lake Image* (512 × 512) pixels, considering upscale factor of 3 and dictionary size of 512. (a) Original image, (b) Bicubic interpolation, (c) DCT interpolation, (d) SR method proposed in Yang et al (2010) (e) SR method proposed Zeyde et al (2010), (f) Our method SR-1 and (g) Our method SR-2.
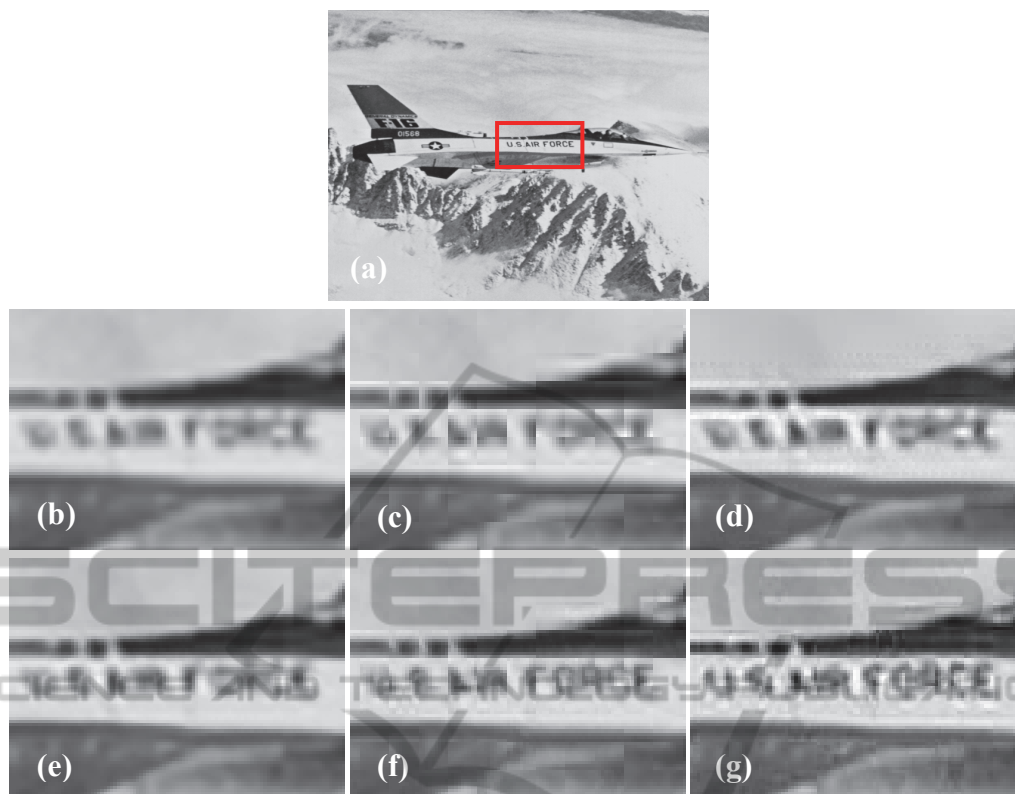
Figure 4: Visual quality results of *Jet plane* image (512×512) pixels, considering upscale factor of 3 and dictionary size of 512. (a) Original Image, (b) Bicubic interpolation, (c) DCT interpolation, (d) SR method Yang et al (2010) (e) SR method Zeyde et al (2010), (f) Our method SR-1 and (g) Our method SR-2.